

Accepted Manuscript

Design, synthesis and biological evaluation of novel spiro-pentacylamides as acetyl-CoA carboxylase inhibitors

Qiangqiang Wei, Liankuo Mei, Yifei Yang, Hui Ma, Hongyi Chen, Huibin Zhang, Jinpei Zhou

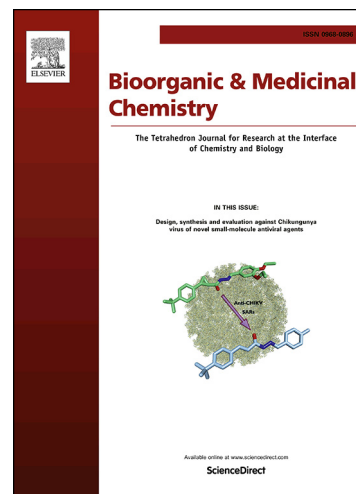
PII: S0968-0896(18)30255-4
DOI: <https://doi.org/10.1016/j.bmc.2018.03.014>
Reference: BMC 14252

To appear in: *Bioorganic & Medicinal Chemistry*

Received Date: 9 February 2018
Revised Date: 7 March 2018
Accepted Date: 8 March 2018

Please cite this article as: Wei, Q., Mei, L., Yang, Y., Ma, H., Chen, H., Zhang, H., Zhou, J., Design, synthesis and biological evaluation of novel spiro-pentacylamides as acetyl-CoA carboxylase inhibitors, *Bioorganic & Medicinal Chemistry* (2018), doi: <https://doi.org/10.1016/j.bmc.2018.03.014>

This is a PDF file of an unedited manuscript that has been accepted for publication. As a service to our customers we are providing this early version of the manuscript. The manuscript will undergo copyediting, typesetting, and review of the resulting proof before it is published in its final form. Please note that during the production process errors may be discovered which could affect the content, and all legal disclaimers that apply to the journal pertain.



Design, synthesis and biological evaluation of novel spiro-pentacylamides as acetyl-CoA carboxylase inhibitors

Qiangqiang Wei^a, Liankuo Mei^b, Yifei Yang^a, Hui Ma^b, Hongyi Chen^a, Huibin Zhang^{b*}, Jinpei Zhou^{a*}

^a Department of Medicinal Chemistry, China Pharmaceutical University, 24 Tongjiaxiang, Nanjing 210009, PR China

^b Center of Drug Discovery, State Key Laboratory of Natural Medicines, China Pharmaceutical University, 24 Tongjiaxiang, Nanjing 210009, PR China[†]

Abstract

Acetyl-CoA carboxylase (ACC) catalyzes the rate-determining step in de novo lipogenesis and plays an important role in the regulation of fatty acid oxidation. Therefore, ACC inhibition offers a promising option for intervention in nonalcoholic fatty liver disease (NAFLD), type 2 diabetes (T2DM) and cancer. In this paper, a series of spiro-pentacylamide derivatives were synthesized and evaluated for their ACC1/2 inhibitory activities and anti-proliferation effects on A549, H1975, HCT116, SW620 and Caco-2 cell lines *in vitro*. Compound **60** displayed potent ACC1/2 inhibitory activity (ACC1 IC₅₀ = 0.527 μM, ACC2 IC₅₀ = 0.397 μM) and the most potent anti-proliferation activities against A549, H1975, HCT116, SW620 and Caco-2 cell lines, with IC₅₀ values of 1.92 μM, 0.38 μM, 1.22 μM, 2.05 μM and 5.42 μM respectively. Further molecular docking studies revealed that compound **60** maintained hydrogen bonds between the two carbonyls and protein backbone NHs (Glu-B2026 and Gly-B1958). These results indicate that compound **60** is a promising ACC1/2 inhibitor for the potent treatment of cancer.

1. Introduction

In contrast to normal differentiated cells, which satisfy their requirement for fatty acids by importing them from the circulation, cancer cells undergo high rates of de novo lipogenesis (DNL) to support cell division and continuous proliferation^[1, 2]. A wide number of cancers such as those of the prostate^[3], hepatoma^[4], bladder, lung, colon and ovary^[5] have been shown to have a high rate of fatty acid synthesis (FASyn) which is reflected by the increased expression of lipogenic enzymes^[6-9]. Modulation of lipogenic enzymes such as cytoplasmic acetyl-CoA synthetase (ACSS2)^[10, 11], ATP citrate lyase (ACLY)^[12], acetyl-CoA carboxylase (ACC)^[13-15] and fatty acid synthase (FASN)^[16] have demonstrated inhibition of cell growth and proliferation in cancer models both *in vitro* and *in vivo*.

Acetyl-CoA carboxylase (ACC) is a biotin-dependent protein, composed of a carboxyl transferase domain (CT), biotin carboxy carrier protein (BCCP) and biotin carboxylase domain (BC), which catalyzes the ATP-dependent carboxylation of acetyl-CoA to form malonyl-CoA, the rate-limiting and first committed reaction in FASyn^[17, 18]. There are two characterized isoforms of

[†]* Corresponding authors. Center of Drug Discovery, State Key Laboratory of Natural Medicines, China Pharmaceutical University, 24 Tongjiaxiang, Nanjing 210009, China. Tel: +86-25-83271302; Fax: +86-25-83271480. E-mail: zhanghb80@cpu.edu.cn

* Corresponding authors. Department of Medicinal Chemistry, China Pharmaceutical University, 24 Tongjiaxiang, Nanjing 210009, PR China. Tel: +86-25-83271302; Fax: +86-25-83271480. E-mail: jpzhou668@163.com

mammalian ACC (known as ACC1 and ACC2), which are encoded by separate genes and display distinct cellular distributions^[19]. ACC1 is located in the cytosol and primarily expressed in lipid rich tissues (liver, adipose)^[20]. In contrast, the second ACC isoform, ACC2 is a mitochondrially associated isozyme present in oxidative tissues (heart, skeletal muscle)^[21]. ACC1 converts acetyl-CoA into malonyl-CoA for DNL while the ACC2 isoform carries out the same reaction to generate malonyl-CoA for the inhibition of carnitine palmitoyl transferase 1 (CPT-1)^[22], the protein that catalyzes the conjugation of free fatty acyls to carnitine from entering the mitochondrial membrane for subsequent β -oxidation^[23]. Thus, malonyl-CoA production by ACC2 activity serves to directly inhibit fatty acid oxidation. Considering the roles of the ACC in both the synthesis and oxidation of fatty acids, inhibition of ACC1/2 has the potential to favorably affect a variety of metabolic diseases including T2DM, obesity and NAFLD by reducing lipid accumulation and improving insulin sensitization^[24, 25]. In addition, given that the tumor cells rely on FASyn for energy storage, membrane formation and production of signaling molecules^[26] and that both ACC and FASN mRNAs are upregulated in a number of cancers, FASyn has been postulated to offer a therapeutic window. In this paper, efforts to target cancer cells that bear elevated rates of lipogenesis have focused on attempts to chemically inhibit ACC1/2.

To date, several classes of small molecule ACC1/2 inhibitors have been reported and the representative structures are presented in **Fig. 1**^[5, 15, 27-29]. Pfizer has had a long-standing interest in the development of ACC inhibitors and reported a series of potent, nonselective and orally bioavailable spirochormanone ACC1/2 dual inhibitors as exemplified by **PF-1** and the co-crystal structure of the humanized yeast ACC carboxyl transferase (CT) domain in complex with **PF-2** was performed (PDB: 4WYO, **Fig. 2**). Compound **PF-2** was oriented in the channel generated at the dimeric interface of the N and C domains, and the pyrazolopyranone group was filling a narrow, deep, hydrophobic pocket formed by a cluster of hydrophobic residues (Leu-A1762, Val-A1765, Leu-A1766, Ala-B1920, Val-B1923, and Phe-B1925) from each domain. The co-crystal data also indicated that the amide carbonyl (right side) interacts with the backbone of Glu-B2026 and the ketone carbonyl (left side) is bound to the backbone of Gly-B1958, which made significant contributions to binding potency. Notably, further co-crystal structure published by Pfizer of compound **PF-3** (**Fig. 2**) demonstrated that the proper fixation of the ketone carbonyl (left side) direction may lead to a nearly identical hydrogen bonding interaction as compared to **PF-2**. In addition, the structural rigidity imparted by the spirocyclic ring system was essential to binding by reducing the entropic penalty for properly orienting the hydrogen bond acceptors^[30]. Herein, we report the discovery of a spiro-lactam derivative **6o** bearing a spiro-pentacylamide ring formed by focusing interactions with Gly-B1958 and Glu-B2026 to explore inhibitory activity of ACC.

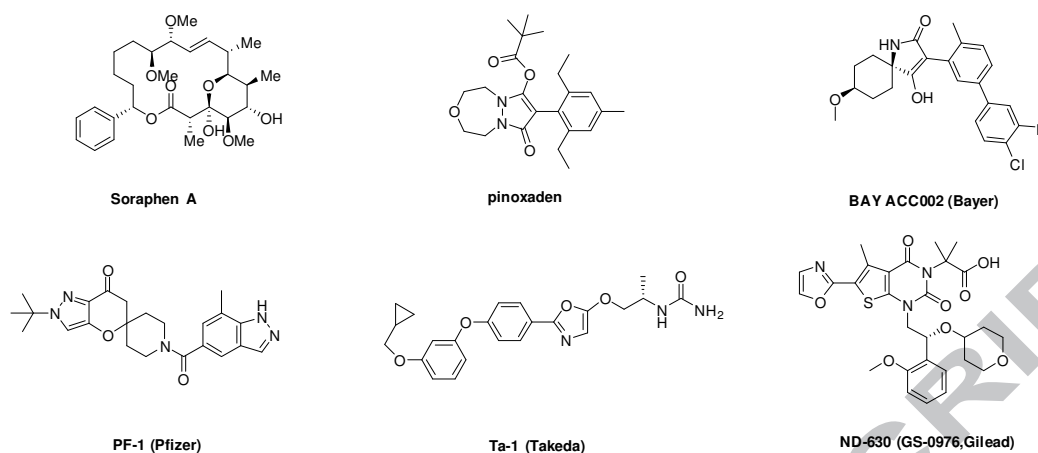


Fig. 1. Representative inhibitors of ACC

On the basis of spirochromanone scaffold reported by Pfizer, our modification strategy was focused on the pyrazolopyranone region of compound **PF-2** as shown in **Fig. 3**. Spatial orientation of the amide carbonyl (right side) and ketone carbonyl (left side) were retained to form the key hydrogen-bonds with Glu-B2026 and Gly-B1958, respectively. On the other hand, we focused on searching for substituents that would provide an optimal fit in the binding pocket composed primarily of hydrophobic side chains. In consideration of the above two points, the spiro-pentacylamide scaffold was designed. Meanwhile a range of phenyl substituents were introduced via standard Buchwald coupling conditions to occupy the hydrophobic pocket.

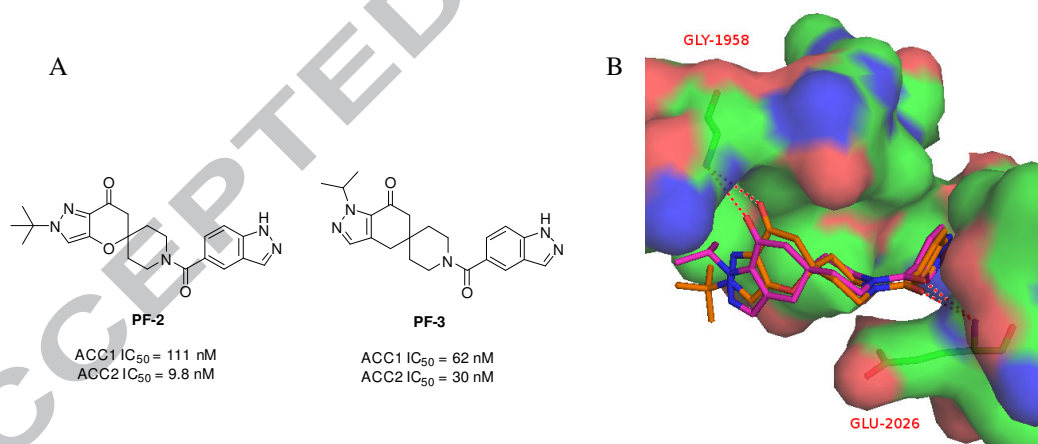


Fig. 2. (A). ACC inhibitors **PF-2** and **PF-3**. (B). Co-crystal structure of **PF-2** (orange) bound in the CT-domain of ACC, overlaid with the bound conformation of **PF-3** (magenta). PDB accession codes: **PF-2**, 4WYO; **PF-3**, 4WZ8.

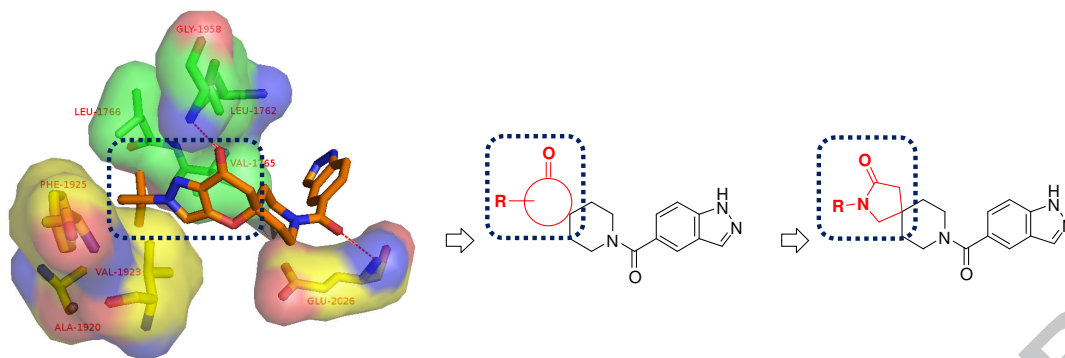
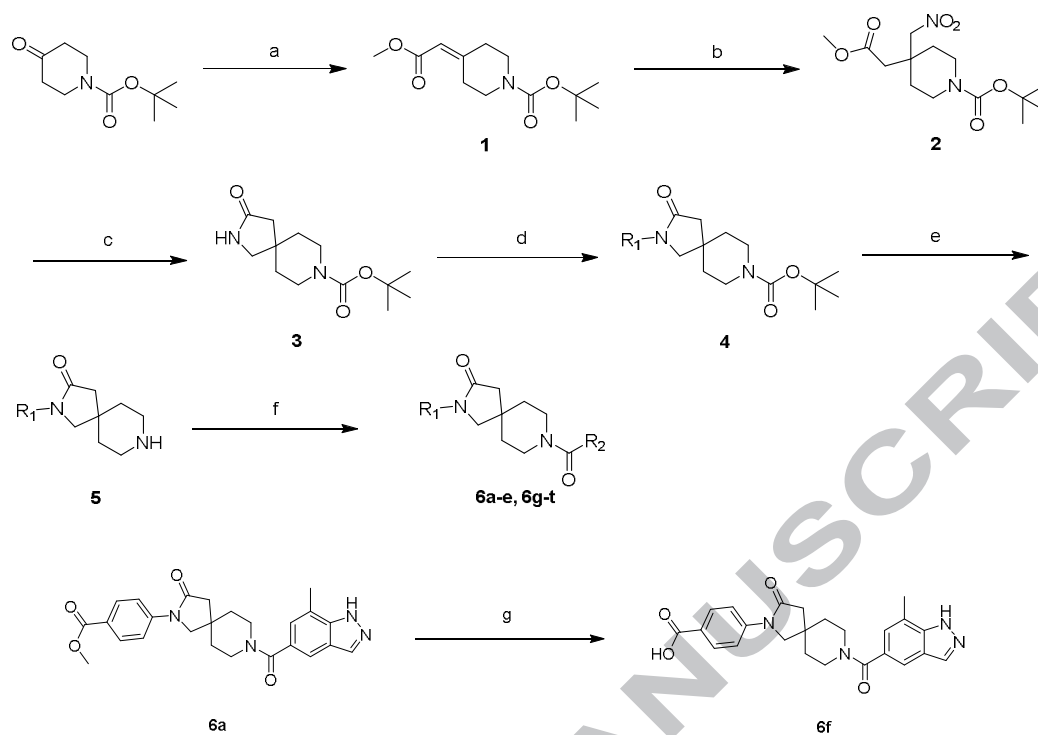


Fig. 3. Design strategy of spiro-pentacylamide derivatives.

Herein, we would like to describe our efforts on the biological evaluation and structural optimization of the novel spiro-pentacylamide-based ACC1/2 inhibitors. The synthesized compounds were evaluated for their biological activities *in vitro* toward five different human tumour cell lines, and ACC enzymes. Among these derivatives, compound **60** with the most potent ACC inhibition activity (ACC1 IC_{50} = 0.527 μ M, ACC2 IC_{50} = 0.397 μ M) and the most potent anti-proliferation activity against A549, H1975, HCT116, SW620 and Caco-2 cell lines (1.92 μ M, 0.38 μ M, 1.22 μ M, 2.05 μ M and 5.42 μ M), respectively, was considered to be a promising lead compound worthy of further investigation. The binding interactions between ACC and compound **60** are presented within this paper as well.

2. Chemistry

The synthetic route with high to moderate yields for accessing the desired compounds **6a-6t** is described in Scheme 1. The commercially available *tert*-butyl 4-oxopiperidine-1-carboxylate and methyl (triphenylphosphoranylidene)acetate were refluxed in toluene to afford **1**^[31]. The intermediate **2** was prepared from **1** using nitromethane in the presence of tetrabutylammonium fluoride (TBAF) in tetrahydrofuran. The key intermediate **3** was obtained by treating **2** with Raney-nickel under an hydrogen atmosphere at room temperature. Next, **3** was subjected to Buchwald-Hartwig *C-N* coupling reaction with substituted bromophenyl reagents in the presence of potassium phosphate and catalytic amount of 4,5-bis(diphenylphosphino)-9,9-dimethylxanthene and palladium catalyst in dioxane at 100°C to give the desired compound **4a-e**^[32]. The removal of the Boc group of **4a-e** by treatment with HCl in ethyl acetate yielded **5a-e** at room temperature. Finally, the target compounds **6a-6e** and **6g-6t** were synthesized by the classical method of amide formation involving condensation between **5a-e** with a variety of carboxylic acid derivatives in dimethylformamide (DMF) under room temperature. In addition, the target compound **6f** was obtained by hydrolysis of compound **6a** with 2 M aqueous NaOH in MeOH/water.



Scheme 1. Synthetic route for target compounds **6a-6t**. Reagents and conditions: (a) methyl (triphenylphosphoranylidene)acetate, toluene, reflux; (b) nitromethane, TBAF, THF, rt-70°C; (c) Raney-Ni, H₂, EtOH, rt; (d) substituted bromophenyl reagents, Pd₂(dba)₃, K₃PO₄, 4,5-bis(diphenylphosphino)-9,9-dimethylxanthene, dioxane, 100°C; (e) (i) HCl gas, ethyl acetate, rt; (ii) 2M aqueous NaOH, H₂O; (f) corresponding carboxylic acid derivatives, 1-hydroxybenzotriazole (HOBt), 1-(3-dimethylaminopropyl)-3-ethylcarbodiimide hydrochloride (EDCI), Et₃N, DMF, 40°C. (g) 2M aqueous NaOH, MeOH/H₂O, 40°C.

3. Results and discussion

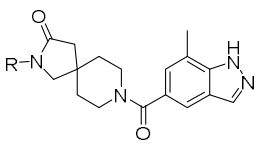
3.1. *In vitro* ACC inhibitory activities

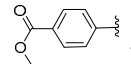
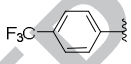
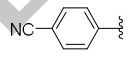
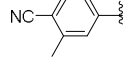
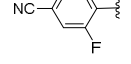
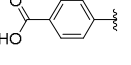
Taking **PF-1** as reference compound, the target compounds **6a-6t** were tested for *in vitro* ACC inhibitory activities and the results are summarized in **Tables 1** and **2**. We initially varied the groups on the *N*-phenyl moiety to afford compounds **6a-6f**. The most potent analog from this work was (trifluoromethyl)phenyl derivative **6b** (ACC1 IC₅₀ = 1.202 μM, ACC2 IC₅₀ = 0.944 μM). Next, we selected the (trifluoromethyl)phenyl as an ‘anchor’ group, and the amide tail region SAR was explored by coupling **5b** to several carboxylic acids and the results are shown in **Table 2**. 5-Carboxybenzimidazole derivatives showed more activity than the indole, indazole and quinoline analogs, which were similar to spirochromanone-based ACC inhibitors reported by Pfizer. Of the three benzimidazole derivatives prepared (**6g**, **6h** and **6o**), **6o** (ACC1 IC₅₀ = 0.527 μM, ACC2 IC₅₀ = 0.397 μM) exhibited the best potency. Therefore, further optimization efforts around the benzimidazole moiety led to the synthesis of compounds **6p-6t**. Unexpectedly, all compounds exhibited modestly lower ACC inhibitory potency than **6o**. To understand the binding mode of this series, we performed docking experiments with Glide docking in Schrodinger. Comparison of the interactions of **PF-2** and **6o** bound in the CT-domain of ACC showed that both molecules

maintained hydrogen bonds between the two carbonyls and protein backbone NHs (**Fig. 4**). Notably, however, the bound position of the carbonyl of **6o** and its hydrogen bond distance (3.7 Å) were clearly distinct from **PF-2**, which may result in lower potency of spiro-pentacylamide derivatives compounds. Another interesting phenomenon observed was that the 2-phenylbenzimidazole moiety of **6o** was directed toward an open pocket formed by backbone atoms of residues Ile-B2033, Glu-B2032, Gly-B2029, Lys-C1954, Ser-C1976 and Gly-C1758 (for clarity, not shown in **Fig. 4**), which may offer a promising option for compound design.

Table 1

Chemical structures of target compounds **6a-6f** and their ACC inhibitory activities.



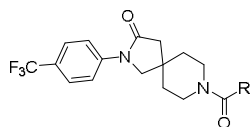
Compound	R	IC ₅₀ (μM) ^a	
		ACC1	ACC2
6a		2.241±0.013	1.882±0.019
6b		1.202±0.006	0.944±0.017
6c		3.990±0.024	> 5
6d		2.011±0.022	3.772±0.024
6e		3.559±0.018	> 5
6f		2.792±0.011	4.646±0.009
PF-1^b		0.032±0.009	0.008±0.013

^a IC₅₀ values for ACC1 and ACC2 activities presented are the mean ± SD values of three independent determinations

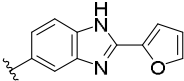
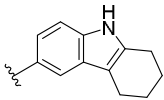
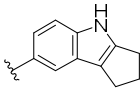
^b Used as positive control.

Table 2

Chemical structures of target compounds **6g-6t** and their ACC inhibitory activities.



Compound	R	IC ₅₀ (μM) ^a	
		ACC1	ACC2
6g		2.221±0.008	3.021±0.0012
6h		1.687±0.017	1.944±0.006
6i		> 5	> 5
6j		4.955±0.015	> 5
6k		4.726±0.009	2.738±0.019
6l		4.923±0.016	> 5
6m		> 5	> 5
6n		> 5	> 5
6o		0.527±0.022	0.397±0.014
6p		1.147±0.013	0.764±0.015
6q		2.649±0.016	1.237±0.024

6r		1.054±0.021	0.976±0.006
6s		1.948±0.022	1.112±0.019
6t		4.265±0.018	3.477±0.023
PF-1^b		0.056±0.011	0.014±0.015

^a IC₅₀ values for ACC1 and ACC2 activities presented are the mean ± SD values of three independent determinations

^b Used as positive control.

3.2. Anticancer evaluation against cancer cell lines in vitro

The anti-proliferation activity of the compounds was screened against A549, H1975, HCT116, SW620 and Caco-2 cell lines using the MTT assay. ACC1 was highly expressed in all five cell lines^[13], and ACC2 had expression levels ranging from low to undetectable. The bioactivity data is summarized in **Table 3**. Compound **PF-1** was used as positive control.

As illustrated in **Table 3**, most of the target compounds **6a–b**, **6h**, **6o–s** were shown to have anti-proliferation activities. Overall, all the compounds showed higher activity against H1975 cell line and moderate activity against A549 cell line, but lower activity against HCT116, SW620 and Caco-2 cell lines. Two selected compounds (**6h** and **6o**) showed comparable activity against H1975, HCT116 and SW620 cells lines with the positive drug **PF-1**. The most promising compound **6o** exhibited the best activity against A549, H1975, HCT116, SW620 and Caco-2 cell lines with the IC₅₀ values of 1.92 μM, 0.38 μM, 1.22 μM, 2.05 μM and 5.42 μM respectively. These results indicated that compound **6o** could be a promising lead compound for anti-cancer.

Table 3

The anti-proliferation activities of **6a–o** against A549, H1975, HCT116, SW620 and Caco-2 cell lines in vitro.

Compound	IC ₅₀ (μM) ^a				
	A549	H1975	HCT116	SW620	Caco-2
6a	2.11±0.41	5.64±0.81	>10	>10	>10
6b	>10	>10	8.67±2.78	>10	>10
6h	>10	0.27±0.02	4.21±0.17	1.82±0.61	>10
6o	1.92±0.05	0.38±0.03	1.22±0.11	2.05±0.07	5.42±0.69
6p	1.03±0.73	>10	6.21±0.25	>10	>10
6q	3.49±0.94	0.39±1.22	7.64±1.49	7.24±1.91	>10
6r	7.96±0.13	0.72±0.98	>10±0.63	3.26±1.11	n.d. ^b
6s	>10	n.d.	8.67±0.18	4.74±0.94	n.d.
PF-1^c	0.74±0.22	0.21±0.05	2.43±0.44	3.19±0.49	6.51±2.12

^a The data were expressed as the means ± SD, representing the relative levels of anti-proliferation from three independent experiments.

^b n.d. = not determined.

^c Used as positive control.

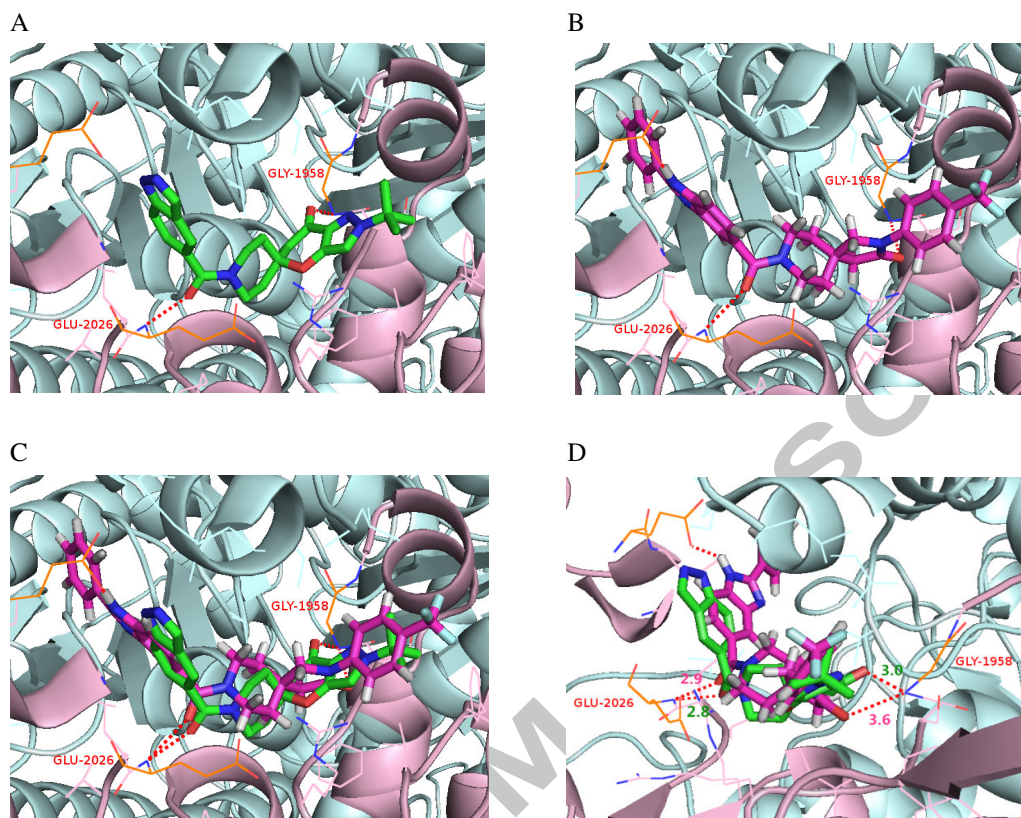


Fig. 3 (A) Docking conformation of **PF-2** with ACC CT domain (PDB id: 4WYO). (B) Docking conformation of **6o** with ACC CT domain. (C) (D) Superimposition docking conformation of **PF-3** (Green) and **6o** (Pink) with ACC CT domain.

4. Conclusions

In summary, on the basis of the spiroketone scaffold reported by Pfizer, we designed and synthesized a series of novel spiro-pentacylamide derivatives as ACC inhibitors. All the compounds were initially screened for ACC enzyme inhibition and some selected compounds were further evaluated for the activity against A549, H1975, HCT116, SW620 and Caco-2 cell lines. Two compounds (**6h** and **6o**) showed comparable activity against H1975, HCT116 and SW620 cells lines with the positive control **PF-1**. The most promising compound, **6o** (ACC1 IC_{50} = 0.527 μ M, ACC2 IC_{50} = 0.397 μ M), had IC_{50} values of 1.92 μ M, 0.38 μ M, 1.22 μ M, 2.05 μ M and 5.42 μ M against A549, H1975, HCT116, SW620 and Caco-2 cell lines, respectively. Moreover, SAR study indicated that substituting group at the 2-position on the terminal benzimidazole ring was beneficial in terms of ACC inhibitory and anti-proliferation activities. Furthermore, docking studies demonstrated that compound **6o** formed the key hydrogen-bonds with Glu-B2026 and Gly-B1958. Combined results from enzymatic assays and molecular docking analysis therefore indicated that compound **6o** was a potent ACC inhibitor and ACC inhibition, by reducing DNL and increasing mitochondrial oxidation rates, may have therapeutic utility for the suppression of tumor growth. The structural modification of **6o** as well as the SAR will be carried

out in the follow-up study.

5. Experimental section

5.1. General information

Solvents and reagents were purchased from Bide Pharmatech Ltd., Energy Chemical, Accela ChemBio Co., Ltd., Shanghai Chemical Reagent Co., Ltd., and TCI, and were used without further purification. Reaction progress was monitored by TLC using HSGF 254 (150–200 μ m thickness; Yantai Jiangyou Co., China) with detection by UV. Silica gel 200-300 was used for column chromatography. ^1H NMR and ^{13}C NMR spectra were recorded on Bruker AV-300 spectrometer at 25 $^\circ\text{C}$ and referenced to TMS. Chemical shifts were given in ppm (δ) downfield from tetramethylsilane. Proton coupling patterns were described as singlet (s), doublet (d), triplet (t), quartet (q), multiplet (m), and broad (br). Melting points were measured on capillary tube and were uncorrected. Purity of the target compounds were determined by HPLC analysis (UV detector, wavelength: 272 nm). Mass spectrometry (MS) was performed using an Hewlett-Packard 1100 LC/MSD spectrometer;

5.2. Chemical synthesis

5.2.1. *tert*-Butyl 4-(2-methoxy-2-oxoethylidene)piperidine-1-carboxylate (**1**)

A solution of *tert*-butyl *tert*-butyl 4-oxopiperidine-1-carboxylate (5 g, 25.1 mmol) and methyl (triphenylphosphoranyl)acetate (8.4 g, 25.1 mmol) in toluene (100 mL) was heated to reflux and stirred for 17 h. The reaction mixture was then cooled to room temperature and evaporated under reduced pressure and purified by silica gel column chromatography, eluting with DCM/petroleum ether (1/1, v/v) to obtain **1** as a white solid (5.44 g, 85% yield). ^1H NMR (300 MHz, CDCl_3) δ 5.72 (s, 1H), 3.70 (s, 3H), 3.50 (dd, $J = 12.6, 7.2$ Hz, 4H), 2.94 (t, $J = 5.6$ Hz, 2H), 2.33 – 2.22 (m, 2H), 1.49 (d, $J = 6.5$ Hz, 9H).

5.2.2. *tert*-Butyl 4-(2-methoxy-2-oxoethyl)-4-(nitromethyl)piperidine-1-carboxylate (**2**)

To a stirred solution of compound **1** (4 g, 15.62 mmol) and nitro methane (1.05 g, 17.22 mmol) in THF (20 mL), 1.0 M solution of TBAF in THF (23.53 mL, 23.53 mmol) was added drop wise at 0 $^\circ\text{C}$ for 20 min. The reaction mixture was refluxed at 70 $^\circ\text{C}$ for 16 h. The reaction mixture was partitioned between H_2O and ethyl acetate, and the organic layers were combined and dried (Na_2SO_4). The solvent was removed *in vacuo* and the residue was purified by column chromatography (0 to 30% EtOAc in petroleum ether) to afford **2** as a white solid (3.79 g, 76% yield). ^1H NMR (300 MHz, DMSO) δ 4.77 (s, 2H), 3.60 (s, 3H), 3.49 – 3.27 (m, 4H), 2.58 (s, 2H), 1.67 – 1.47 (m, 4H), 1.39 (s, 9H).

5.2.3. *tert*-Butyl 3-oxo-2,8-diazaspiro[4.5]decane-8-carboxylate (**3**)

A mixture of compound **2** (3 g, 9.45 mmol) and Ranet-nickel (4 g) in 50 mL EtOH was stirred under hydrogen at room temperature for 12 h. The reaction mixture was filtered through Celite, washed with EtOH and the filtrate was evaporated to afford compound **3** as an off-white solid (1.95 g, 81% yield). ^1H NMR (300 MHz, CDCl_3) δ 6.19 (s, 1H), 3.60 – 3.43 (m, 2H), 3.38 – 3.24 (m, 2H), 3.22 (s, 2H), 2.25 (s, 2H), 1.62 (t, $J = 5.2$ Hz, 4H), 1.47 (s, 9H).

5.2.4. General procedure for preparation of intermediates (4a–e)

To a round bottom flask was added compound **3** (0.5 g, 1.97 mmol), K₃PO₄ (1.25 g, 5.9 mmol), Pd₂(dba)₃ (0.018 g, 0.02 mmol), 9,9-dimethyl-4,5-bis(diphenylphosphino)-xanthene (0.023 g, 0.039 mmol), corresponding bromophenyl substituents (2.36 mmol) and 10 mL dioxane. The reaction mixture was thoroughly degassed with nitrogen, and heated at 100 °C overnight. After cooling to room temperature, the reaction mixture was partitioned between H₂O and ethyl acetate. The organic layers were combined and concentrated. The resulting crude material was purified via silica gel chromatography by eluting with a gradient of 1:3 to 2:1 ethyl acetate/ petroleum ether to give the title compounds **4a–e**.

5.2.4.1. *tert*-Butyl 2-(4-(methoxycarbonyl)phenyl)-3-oxo-2,8-diazaspiro[4.5]decane-8-carboxylate (**4a**). Off white solid, yield 88%; ¹H NMR (300 MHz, CDCl₃) δ 8.06 (d, *J* = 7 Hz, 2H), 7.73 (d, *J* = 8.9 Hz, 2H), 3.93 (s, 3H), 3.71 (s, 2H), 3.64 (b, 2H), 3.35 (m, 2H), 2.59 (s, 2H), 1.71 (m, 4H), 1.49 (s, 9H).

5.2.4.2. *tert*-Butyl 3-oxo-2-(4-(trifluoromethyl)phenyl)-2,8-diazaspiro[4.5]decane-8-carboxylate (**4f**). White solid, yield 91%; ¹H NMR (300 MHz, CDCl₃) δ 7.76 (d, *J* = 7.6 Hz, 2H), 7.64 (d, *J* = 7.6 Hz, 2H), 3.69 (s, 4H), 3.33 (d, *J* = 7.0 Hz, 2H), 2.58 (s, 2H), 1.69 (s, 4H), 1.50 (s, 10H).

5.2.4.3. *tert*-Butyl 2-(4-cyanophenyl)-3-oxo-2,8-diazaspiro[4.5]decane-8-carboxylate (**4c**). White solid, yield 89%; ¹H NMR (300 MHz, CDCl₃) δ 7.77 (d, *J* = 8.9 Hz, 2H), 7.65 (d, *J* = 8.9 Hz, 2H), 3.70 – 3.55 (m, 4H), 3.37 – 3.23 (m, 2H), 2.58 (s, 2H), 1.68 (t, *J* = 5.6 Hz, 4H), 1.47 (s, 10H).

5.2.4.4. *tert*-Butyl 2-(4-cyano-3-methylphenyl)-3-oxo-2,8-diazaspiro[4.5]decane-8-carboxylate (**4d**). White solid, yield 80%; ¹H NMR (300 MHz, CDCl₃) δ 7.66 – 7.53 (m, 3H), 3.68 – 3.56 (m, 4H), 3.36 – 3.24 (m, 2H), 2.57 (d, *J* = 5.3 Hz, 5H), 1.68 (t, *J* = 5.6 Hz, 4H), 1.47 (s, 9H).

5.2.4.5. *tert*-Butyl 2-(4-cyano-2-fluorophenyl)-3-oxo-2,8-diazaspiro[4.5]decane-8-carboxylate (**4e**). White solid, yield 85%; ¹H NMR (300 MHz, CDCl₃) δ 7.85 (dd, *J* = 7.0, 1.9 Hz, 1H), 7.58 (ddd, *J* = 8.6, 4.5, 2.1 Hz, 1H), 7.31 (s, 1H), 3.67 (s, 2H), 3.62 – 3.49 (m, 2H), 3.48 – 3.29 (m, 2H), 2.52 (s, 2H), 1.70 (dd, *J* = 12.1, 6.3 Hz, 4H), 1.48 (s, 9H).

5.2.5. General procedure for preparation of intermediates (5a–e)

To a solution of an appropriate intermediates **4a–e** (2 mmol) in ethyl acetate (5 mL) was added 4 N HCl in ethyl acetate (10 mL), and the resulting mixture was stirred at room temperature for 2 h. The resulting precipitate was collected by filtration and washed with ethyl acetate. Subsequently, the precipitate was resolved and neutralized to afford the target compounds **4a–e** as an off white solid.

5.2.5.1. Methyl 4-(3-oxo-2,8-diazaspiro[4.5]decan-2-yl)benzoate (**5a**) Off-white solid, yield 91%; ¹H NMR (300 MHz, DMSO-*d*₆) δ 7.96 (d, *J* = 8.9 Hz, 2H), 7.83 (d, *J* = 8.9 Hz, 2H), 3.83 (s, 3H), 3.69 (s, 2H), 2.81 – 2.59 (m, *J* = 14.3 Hz, 4H), 2.48 (s, 2H), 1.49 (m, *J* = 14.3 Hz, 4H).

5.2.5.2. 2-(4-(Trifluoromethyl)phenyl)-2,8-diazaspiro[4.5]decan-3-one (**5b**) White solid, yield

88%; ^1H NMR (300 MHz, DMSO- d_6) δ 7.90 (d, J = 8.3 Hz, 2H), 7.76 (d, J = 8.3 Hz, 2H), 3.81 (s, 2H), 3.07 (m, J = 12.3 Hz, 4H), 2.61 (s, 2H), 1.85 (m, J = 12.3 Hz, 4H).

5.2.5.3. 4-(3-Oxo-2,8-diazaspiro[4.5]decan-2-yl)benzotrile (5c) Off white solid, yield 80%; ^1H NMR (300 MHz, DMSO- d_6) δ 7.86 (dd, J = 16.2, 8.0 Hz, 4H), 3.69 (s, 2H), 2.67 (m, J = 5.2 Hz, 4H), 2.43 (s, 2H), 1.50 (m, J = 5.2 Hz, 4H).

5.2.5.4. 2-Methyl-4-(3-oxo-2,8-diazaspiro[4.5]decan-2-yl)benzotrile (5d) Off white solid, yield 90%; ^1H NMR (300 MHz, DMSO- d_6) δ 7.83 – 7.64 (m, 3H), 3.65 (s, 2H), 2.65 (m, J = 12.6, 6.4 Hz, 4H), 2.46 (s, 5H), 1.48 (m, J = 5.0 Hz, 4H).

5.2.5.5. 3-Fluoro-4-(3-oxo-2,8-diazaspiro[4.5]decan-2-yl)benzotrile (5e) White solid, yield 81%; ^1H NMR (300 MHz, DMSO- d_6) δ 7.84 – 7.66 (m, 3H), 3.61 (s, 2H), 2.62 (m, J = 13.9 Hz, 4H), 2.42 (s, 2H), 1.46 (m, J = 13.9 Hz, 4H).

5.2.6. General procedure for preparation of target compounds (6a–6e, 6g–6t)

A mixture of intermediates **4a–e** (0.60 mmol), EDCI (138 mg, 0.72 mmol), corresponding carboxylic acid derivatives (0.60 mmol) and HOBt (97 mg, 0.72 mmol) in *N,N*-dimethylformamide (6.0 mL) was stirred for 20 h. The reaction mixture was diluted with ethyl acetate and washed with brine, the organic layer was dried over magnesium sulfate and concentration *in vacuo*. The residue was purified by silica gel column chromatography (5% methanol/chloroform) to afford the title compounds **6a–t** as a white solid.

5.2.6.1.

Methyl

4-(8-(7-methyl-1H-indazole-5-carbonyl)-3-oxo-2,8-diazaspiro[4.5]decan-2-yl)benzoate (**6a**)

White solid; yield 70%; m.p.: 199–201 °C; ^1H NMR (300 MHz, DMSO- d_6) δ 13.35 (s, 1H), 8.13 (s, 1H), 7.97 (d, J = 8.9 Hz, 2H), 7.82 (d, J = 8.9 Hz, 2H), 7.64 (s, 1H), 7.16 (s, 1H), 3.83 (s, 3H), 3.78 (s, 2H), 3.49 (m, 4H), 2.59 (s, 2H), 2.54 (s, 3H), 1.65 (s, 4H). ^{13}C NMR (75 MHz, DMSO- d_6) δ 173.1, 169.6, 165.7, 143.6, 140.1, 134.5, 129.9, 128.5, 124.7, 124.3, 121.8, 120.2, 118.5, 116.9, 57.6, 51.9, 43.6, 34.2, 16.7. ESIMS m/z $[\text{M} + \text{H}]^+$ 447.1; Anal. calcd. For $\text{C}_{25}\text{H}_{26}\text{N}_4\text{O}_4$: C, 67.25; H, 5.87; N, 12.55. Found: C, 67.29; H, 5.85; N, 12.51.

5.2.6.2.

3-Fluoro-4-(8-(7-methyl-1H-indazole-5-carbonyl)-3-oxo-2,8-diazaspiro[4.5]decan-2-yl)benzotrile

(**6b**) White solid; yield 81%; m.p.: 221–223 °C; ^1H NMR (300 MHz, DMSO- d_6) δ 13.35 (s, 1H), 8.14 (s, 1H), 7.86 (d, J = 5.4 Hz, 4H), 7.64 (s, 1H), 7.16 (s, 1H), 3.78 (s, 2H), 3.69 – 3.39 (m, 4H), 2.60 (s, 2H), 2.51 (s, 3H), 1.65 (s, 4H). ^{13}C NMR (75 MHz, DMSO- d_6) δ 173.1, 169.6, 142.8, 140.1, 134.5, 128.5, 125.8, 125.8, 124.7, 121.8, 120.2, 119.1, 116.9, 57.6, 43.6, 34.3, 16.7. ESIMS m/z $[\text{M} + \text{H}]^+$ 457.1; Anal. calcd. For $\text{C}_{24}\text{H}_{23}\text{F}_3\text{N}_4\text{O}_2$: C, 63.15; H, 5.08; N, 12.27. Found: C, 63.11; H, 5.12; N, 12.24.

5.2.6.3.

4-(8-(7-Methyl-1H-indazole-5-carbonyl)-3-oxo-2,8-diazaspiro[4.5]decan-2-yl)benzotrile (**6c**)

White solid; yield 90%; m.p.: 217–219°C; ¹H NMR (300 MHz, DMSO-*d*₆) δ 13.36 (s, 1H), 8.14 (s, 1H), 7.89 (d, *J* = 8.8 Hz, 2H), 7.75 (d, *J* = 8.7 Hz, 2H), 7.65 (s, 1H), 7.16 (s, 1H), 3.79 (s, 2H), 3.42 (s, 2H), 3.33 (s, 2H), 2.60 (s, 2H), 2.55 (s, 3H), 1.67 (s, 4H). ¹³C NMR (75 MHz, DMSO-*d*₆) δ 173.4, 169.6, 143.3, 140.1, 134.5, 132.9, 128.4, 124.7, 121.8, 120.2, 119.1, 118.9, 116.9, 105.4, 57.5, 43.6, 34.2, 16.7. ESIMS *m/z* [M + H]⁺ 414.1; Anal. calcd. For C₂₄H₂₃N₅O₂: C, 69.72; H, 5.61; N, 16.94. Found: C, 69.69; H, 5.65; N, 16.97.

5.2.6.4.

*2-Methyl-4-(8-(7-methyl-1H-indazole-5-carbonyl)-3-oxo-2,8-diazaspiro[4.5]decan-2-yl)benzoni-
le (6d)* White solid; yield 72%; m.p.: 237–239°C; ¹H NMR (300 MHz, DMSO-*d*₆) δ 13.35 (s, 1H), 8.13 (s, 1H), 7.75 (s, 2H), 7.71 (s, 1H), 7.64 (s, 1H), 7.16 (s, 1H), 3.76 (s, 2H), 3.66 – 3.40 (m, 4H), 2.58 (s, 2H), 2.54 (s, 3H), 2.47 (s, 3H), 1.65 (s, 4H). ¹³C NMR (75 MHz, DMSO-*d*₆) δ 173.3, 169.6, 143.1, 142.3, 140.1, 134.5, 133.1, 128.4, 124.7, 121.8, 120.2, 119.8, 118.1, 116.9, 116.7, 106.0, 57.5, 43.7, 34.2, 20.2, 16.7. ESIMS *m/z* [M + H]⁺ 428.1; Anal. calcd. For C₂₅H₂₂N₄O₆S₃: C, 70.24; H, 5.89; N, 16.38. Found: C, 70.25; H, 5.92; N, 16.43.

5.2.6.5.

*3-Fluoro-4-(8-(7-methyl-1H-indazole-5-carbonyl)-3-oxo-2,8-diazaspiro[4.5]decan-2-yl)benzoni-
le (6e)* White solid; yield 65%; m.p.: 241–243°C; ¹H NMR (300 MHz, DMSO-*d*₆) δ 13.37 (s, 1H), 8.15 (s, 1H), 8.10 (d, *J* = 6.9 Hz, 1H), 7.87 (d, *J* = 6.8 Hz, 1H), 7.66 (s, 1H), 7.59 (t, *J* = 9.6 Hz, 1H), 7.18 (s, 1H), 3.72 (s, 2H), 3.52 (s, 4H), 2.56 (s, 3H), 2.52 (s, 2H), 1.71 (s, 4H). ¹³C NMR (75 MHz, DMSO-*d*₆) δ 172.4, 169.6, 160.8, 157.4, 140.1, 134.5, 132.7, 131.8, 131.8, 128.5, 127.7, 124.7, 121.8, 120.1, 118.4, 118.1, 117.5, 116.9, 107.8, 107.8, 58.8, 58.7, 36.1, 16.7. ESIMS *m/z* [M + H]⁺ 432.1; Anal. calcd. For C₂₄H₂₂FN₅O₂: C, 66.81; H, 5.14; N, 16.23. Found: C, 66.79; H, 5.15; N, 16.21.

5.2.6.6.

*8-(2-Methyl-1H-benzo[d]imidazole-5-carbonyl)-2-(4-(trifluoromethyl)phenyl)-2,8-diazaspiro[4.5]
decan-3-one (6g)* White solid; yield 75%; m.p.: 203–205°C; ¹H NMR (300 MHz, DMSO-*d*₆) δ 12.47 (s, 1H), 7.87 (d, *J* = 8.5 Hz, 2H), 7.72 (d, *J* = 8.6 Hz, 2H), 7.62 – 7.41 (m, 2H), 7.15 (dd, *J* = 8.3, 1.5 Hz, 1H), 3.77 (s, 2H), 3.46 (s, 4H), 2.57 (s, 2H), 2.50 (s, 3H), 1.64 (s, 4H). ¹³C NMR (75 MHz, DMSO-*d*₆) δ 173.1, 169.8, 153.1, 142.8, 129.1, 125.84, 125.8, 125.7, 123.9, 123.5, 122.5, 120.4, 119.1, 57.6, 43.6, 34.3, 14.6. ESIMS *m/z* [M + H]⁺ 457.1; Anal. calcd. For C₂₄H₂₃F₃N₄O₂: C, 63.15; H, 5.08; N, 12.27. Found: C, 63.21; H, 5.04; N, 12.29.

5.2.6.7.

*8-(7-Methyl-2-propyl-1H-benzo[d]imidazole-5-carbonyl)-2-(4-(trifluoromethyl)phenyl)-2,8-diazas-
piro[4.5]decan-3-one (6h)* White solid; yield 85%; m.p.: 234–236°C; ¹H NMR (300 MHz, DMSO-*d*₆) δ 7.88 (d, *J* = 8.5 Hz, 2H), 7.73 (d, *J* = 8.5 Hz, 2H), 7.32 (s, 1H), 6.97 (s, 1H), 3.78 (s, 2H), 3.55 (d, *J* = 44.3 Hz, 4H), 2.80 (t, *J* = 7.5 Hz, 2H), 2.58 (s, 2H), 2.50 (s, 3H), 1.80 (q, *J* = 7.4 Hz, 2H), 1.65 (s, 4H), 0.95 (t, *J* = 7.3 Hz, 3H). ¹³C NMR (75 MHz, DMSO-*d*₆) δ 173.1, 167.0, 156.0, 142.8, 129.0, 126.1, 125.8, 125.8, 123.9, 123.5, 120.7, 119.1, 57.6, 43.6, 34.3, 30.5, 21.0, 16.7, 13.7. ESIMS *m/z* [M + H]⁺ 499.2; Anal. calcd. For C₂₇H₂₉F₃N₄O₂: C, 65.05; H, 5.86; N, 11.24. Found: C, 65.01; H, 5.82; N, 11.25.

5.2.6.8. 8-(1*H*-Indole-5-carbonyl)-2-(4-(trifluoromethyl)phenyl)-2,8-diazaspiro[4.5]decan-3-one (**6i**) White solid; yield 78%; m.p.: 2432-234°C; ¹H NMR (300 MHz, DMSO-*d*₆) δ 11.27 (s, 1H), 7.89 (d, *J* = 8.6 Hz, 2H), 7.73 (d, *J* = 8.6 Hz, 2H), 7.66 – 7.58 (m, 1H), 7.53 – 7.40 (m, 2H), 7.13 (dd, *J* = 8.3, 1.6 Hz, 1H), 6.49 (ddd, *J* = 3.0, 1.9, 0.9 Hz, 1H), 3.78 (s, 2H), 3.57 (d, *J* = 43.6 Hz, 4H), 2.59 (s, 2H), 1.65 (d, *J* = 6.7 Hz, 4H). ¹³C NMR (75 MHz, DMSO-*d*₆) δ 173.1, 170.5, 142.8, 136.2, 126.9, 126.6, 126.5, 125.8, 125.8, 125.8, 125.7, 123.9, 123.4, 120.2, 119.2, 119.1, 111.1, 101.6, 57.6, 43.6, 34.3, 14.0. ESIMS *m/z* [M + H]⁺ 442.2; Anal. calcd. For C₂₄H₂₂F₃N₃O₂: C, 65.30; H, 5.02; N, 9.52. Found: C, 65.33; H, 5.01; N, 9.55.

5.2.6.9. 8-(1*H*-Indole-6-carbonyl)-2-(4-(trifluoromethyl)phenyl)-2,8-diazaspiro[4.5]decan-3-one (**6j**) White solid; yield 68%; m.p.: 229-231°C; ¹H NMR (300 MHz, DMSO-*d*₆) δ 11.30 (s, 1H), 7.89 (d, *J* = 8.6 Hz, 2H), 7.74 (d, *J* = 8.6 Hz, 2H), 7.58 (d, *J* = 8.1 Hz, 1H), 7.50 – 7.42 (m, 2H), 7.03 (dd, *J* = 8.1, 1.4 Hz, 1H), 6.54 – 6.44 (m, 1H), 3.79 (s, 2H), 3.58 (d, *J* = 51.8 Hz, 4H), 2.60 (s, 2H), 1.66 (s, 4H). ¹³C NMR (75 MHz, DMSO-*d*₆) δ 173.1, 170.3, 142.8, 135.0, 128.5, 128.4, 127.1, 125.9, 125.8, 125.8, 125.7, 119.6, 119.1, 117.8, 110.5, 101.1, 57.6, 43.6, 34.3. ESIMS *m/z* [M + H]⁺ 442.1; Anal. calcd. For C₂₄H₂₂F₃N₃O₂: C, 65.30; H, 5.02; N, 9.52. Found: C, 65.31; H, 5.05; N, 9.51.

5.2.6.10.

8-(1*H*-Indazole-6-carbonyl)-2-(4-(trifluoromethyl)phenyl)-2,8-diazaspiro[4.5]decan-3-one (**6k**) White solid; yield 61%; m.p.: 244–246°C; ¹H NMR (300 MHz, DMSO-*d*₆) δ 13.22 (s, 1H), 8.13 (s, 1H), 7.88 (d, *J* = 8.5 Hz, 2H), 7.82 (d, *J* = 8.3 Hz, 1H), 7.73 (d, *J* = 8.6 Hz, 2H), 7.54 (s, 1H), 7.11 (dd, *J* = 8.3, 1.3 Hz, 1H), 3.79 (s, 2H), 3.49 (s, 4H), 2.59 (s, 2H), 1.68 (s, 4H). ¹³C NMR (75 MHz, DMSO-*d*₆) δ 173.1, 169.2, 142.8, 139.1, 133.8, 133.6, 125.9, 125.8, 125.8, 125.7, 123.0, 120.7, 119.1, 118.9, 108.5, 57.6, 43.6, 34.2. ESIMS *m/z* [M + H]⁺ 443.3; Anal. calcd. For C₂₃H₂₁F₃N₄O₂: C, 62.44; H, 4.78; N, 12.66. Found: C, 62.45; H, 4.75; N, 12.69.

5.2.6.11. 8-(Quinoline-7-carbonyl)-2-(4-(trifluoromethyl)phenyl)-2,8-diazaspiro[4.5]decan-3-one (**6l**) White solid; yield 84%; m.p.: 237-239°C; ¹H NMR (300 MHz, DMSO-*d*₆) δ 8.97 (d, *J* = 3.9 Hz, 1H), 8.42 (d, *J* = 8.3 Hz, 1H), 8.07 (d, *J* = 8.4 Hz, 1H), 8.00 (s, 1H), 7.89 (d, *J* = 8.5 Hz, 2H), 7.73 (d, *J* = 8.6 Hz, 2H), 7.60 (dd, *J* = 8.4, 4.5 Hz, 2H), 3.80 (s, 2H), 3.52 (d, *J* = 67.8 Hz, 3H), 2.60 (s, 2H), 1.71 (s, 4H). ¹³C NMR (75 MHz, DMSO-*d*₆) δ 173.1, 168.2, 151.4, 147.0, 142.8, 137.1, 136.0, 128.6, 128.1, 126.6, 125.9, 125.8, 125.8, 125.7, 124.8, 122.3, 119.1, 57.6, 43.5, 34.2. ESIMS *m/z* [M + H]⁺ 454.1; Anal. calcd. For C₂₅H₂₂F₃N₃O₂: C, 66.22; H, 4.89; N, 9.27. Found: C, 66.21; H, 4.87; N, 9.25.

5.2.6.12. 8-(Quinoline-6-carbonyl)-2-(4-(trifluoromethyl)phenyl)-2,8-diazaspiro[4.5]decan-3-one (**6m**) White solid; yield 77%; m.p.: 216–218°C; ¹H NMR (300 MHz, DMSO-*d*₆) δ 8.96 (dd, *J* = 4.2, 1.7 Hz, 1H), 8.44 (dd, *J* = 8.5, 1.7 Hz, 1H), 8.17 – 7.98 (m, 2H), 7.89 (d, *J* = 8.6 Hz, 2H), 7.84 – 7.67 (m, 3H), 7.59 (dd, *J* = 8.3, 4.2 Hz, 1H), 3.80 (s, 2H), 3.44 (s, 4H), 2.60 (s, 2H), 1.71 (s, 4H). ¹³C NMR (75 MHz, DMSO-*d*₆) δ 173.1, 168.4, 151.5, 147.5, 142.8, 136.5, 134.1, 129.2, 127.8, 127.3, 126.4, 126.1, 125.8, 125.8, 123.9, 123.5, 122.1, 119.1, 57.5, 43.6, 34.2. ESIMS *m/z* [M + H]⁺ 454.2; Anal. calcd. For C₂₅H₂₂F₃N₃O₂: C, 66.22; H, 4.89; N, 9.27. Found: C, 66.23; H, 4.85; N, 9.22.

5.2.6.13. 8-(Quinoline-3-carbonyl)-2-(4-(trifluoromethyl)phenyl)-2,8-diazaspiro[4.5]decan-3-one (**6n**) White solid; yield 74%; m.p.: 239-241°C; ¹H NMR (300 MHz, DMSO-*d*₆) δ 8.92 (d, *J* = 2.2 Hz, 1H), 8.45 (d, *J* = 2.2 Hz, 1H), 8.09 – 8.01 (m, 2H), 7.95 – 7.83 (m, 3H), 7.70 (dd, *J* = 18.6, 8.3 Hz, 3H), 3.80 (s, 4H), 3.49 (s, 4H), 2.61 (s, 2H), 1.72 (s, 4H). ¹³C NMR (75 MHz, DMSO-*d*₆) δ 173.0, 166.7, 148.4, 147.4, 142.8, 134.3, 130.6, 129.1, 128.7, 128.6, 127.3, 126.6, 125.8, 125.8, 119.1, 57.5, 43.5, 34.2. ESIMS *m/z* [M + H]⁺ 454.1; Anal. calcd. For C₂₅H₂₂F₃N₃O₂: C, 66.22; H, 4.89; N, 9.27. Found: C, 66.27; H, 4.84; N, 9.27.

5.2.6.14.

8-(2-Phenyl-1H-benzo[d]imidazole-5-carbonyl)-2-(4-(trifluoromethyl)phenyl)-2,8-diazaspiro[4.5]decan-3-one (**6o**) White solid; yield 80%; m.p.: 212-214°C; ¹H NMR (300 MHz, DMSO-*d*₆) δ 13.11 (s, 1H), 8.29 – 8.10 (m, 2H), 7.89 (d, *J* = 8.5 Hz, 2H), 7.73 (d, *J* = 8.7 Hz, 3H), 7.55 (q, *J* = 9.1, 7.9 Hz, 4H), 7.27 (d, *J* = 9.4 Hz, 1H), 3.79 (s, 2H), 3.59 (d, *J* = 46.5 Hz, 4H), 2.60 (s, 2H), 1.68 (s, 4H). ¹³C NMR (75 MHz, DMSO-*d*₆) δ 173.1, 169.6, 142.8, 140.1, 134.5, 128.4, 125.8, 125.8, 125.7, 125.7, 124.7, 121.8, 120.2, 119.0, 116.9, 57.6, 43.5, 34.2, 16.7. ESIMS *m/z* [M + H]⁺ 519.1; Anal. calcd. For C₂₉H₂₅F₃N₄O₂: C, 67.17; H, 4.86; N, 10.80. Found: C, 67.13; H, 4.88; N, 10.81.

5.2.6.15.

8-(2-(4-Isopropylphenyl)-1H-benzo[d]imidazole-5-carbonyl)-2-(4-(trifluoromethyl)phenyl)-2,8-diazaspiro[4.5]decan-3-one (**6p**) White solid; yield 77%; m.p.: 197-199°C; ¹H NMR (300 MHz, DMSO-*d*₆) δ 13.15 (s, 1H), 8.13 (d, *J* = 8.0 Hz, 2H), 7.88 (d, *J* = 8.6 Hz, 2H), 7.73 (d, *J* = 8.6 Hz, 2H), 7.69 – 7.57 (m, 2H), 7.42 (d, *J* = 8.1 Hz, 2H), 7.25 (d, *J* = 8.3 Hz, 1H), 3.77 (s, 2H), 3.51 (s, 4H), 2.96 (dd, *J* = 13.9, 7.1 Hz, 1H), 2.59 (s, 2H), 1.67 (s, 4H), 1.24-1.24 (m, 6H). ¹³C NMR (75 MHz, DMSO-*d*₆) δ 173.1, 169.7, 152.7, 150.6, 142.7, 127.4, 126.8, 126.6, 125.8, 125.8, 125.7, 125.7, 119.0, 57.6, 43.5, 34.2, 33.3, 31.0, 29.7, 28.9, 23.5. ESIMS *m/z* [M + H]⁺ 561.1; Anal. calcd. For C₃₂H₃₁F₃N₄O₂: C, 68.56; H, 5.57; N, 9.99. Found: C, 68.59; H, 5.58; N, 9.98.

5.2.6.16.

8-(2-(Pyridin-4-yl)-1H-benzo[d]imidazole-5-carbonyl)-2-(4-(trifluoromethyl)phenyl)-2,8-diazaspiro[4.5]decan-3-one (**6q**) White solid; yield 83%; m.p.: 222-224°C; ¹H NMR (300 MHz, DMSO-*d*₆) δ 13.51 (s, 1H), 8.78 (d, *J* = 5.1 Hz, 2H), 8.20 – 8.03 (m, 2H), 7.89 (d, *J* = 8.6 Hz, 2H), 7.74 (d, *J* = 8.7 Hz, 4H), 7.32 (d, *J* = 8.4 Hz, 1H), 3.79 (s, 2H), 3.51 (s, 4H), 2.60 (s, 2H), 1.69 (s, 4H). ¹³C NMR (75 MHz, DMSO-*d*₆) δ 173.1, 169.4, 150.5, 150.2, 142.8, 136.7, 125.8, 125.7, 123.8, 122.7, 121.2, 120.3, 119.0, 117.9, 111.8, 110.6, 57.6, 43.5, 34.2, 31.4, 31.2, 31.0, 28.9. ESIMS *m/z* [M + H]⁺ 520.1; Anal. calcd. For C₂₈H₂₄F₃N₅O₂: C, 64.73; H, 4.66; N, 13.48. Found: C, 64.75; H, 4.67; N, 13.49.

5.2.6.17.

8-(2-(Furan-2-yl)-1H-benzo[d]imidazole-5-carbonyl)-2-(4-(trifluoromethyl)phenyl)-2,8-diazaspiro[4.5]decan-3-one (**6r**) White solid; yield 65%; m.p.: 221-223°C; ¹H NMR (300 MHz, DMSO-*d*₆) δ 13.18 (s, 1H), 7.97 (d, *J* = 1.7 Hz, 1H), 7.89 (d, *J* = 8.6 Hz, 2H), 7.74 (d, *J* = 8.7 Hz, 2H), 7.60 (d, *J* = 8.1 Hz, 2H), 7.25 (p, *J* = 3.0, 2.5 Hz, 2H), 6.75 (dd, *J* = 3.5, 1.8 Hz, 1H), 3.79 (s, 2H), 3.51 (s, 4H), 2.60 (s, 2H), 1.68 (s, 4H). ¹³C NMR (75 MHz, DMSO-*d*₆) δ 173.1, 169.5, 145.1, 144.9, 144.8, 142.8, 130.0, 126.0, 125.8, 125.7, 123.8, 123.4, 122.4, 119.0, 112.3, 111.0, 57.6, 43.6, 34.2, 31.0, 29.7, 28.9. ESIMS *m/z* [M + H]⁺ 509.1; Anal. calcd. For C₂₇H₂₃F₃N₄O₃: C, 63.78; H, 4.56; N, 11.02. Found:

C, 63.79; H, 4.57; N, 11.01.

5.2.6.18.

8-(2,3,4,9-Tetrahydro-1H-carbazole-6-carbonyl)-2-(4-(trifluoromethyl)phenyl)-2,8-diazaspiro[4.5]decan-3-one (**6s**) White solid; yield 80%; m.p.: 204–205°C; ¹H NMR (300 MHz, DMSO-*d*₆) δ 10.89 (s, 1H), 7.89 (d, *J* = 8.5 Hz, 2H), 7.74 (d, *J* = 8.5 Hz, 2H), 7.40 (s, 1H), 7.27 (d, *J* = 8.2 Hz, 1H), 7.05 (dt, *J* = 8.2, 1.6 Hz, 1H), 3.78 (s, 2H), 3.57 (d, *J* = 50.5 Hz, 4H), 2.75 – 2.54 (m, 6H), 1.81 (s, 4H), 1.65 (s, 4H). ¹³C NMR (75 MHz, DMSO-*d*₆) δ 173.1, 170.8, 142.8, 136.0, 135.8, 126.5, 125.84, 125.7, 125.7, 119.3, 119.0, 116.4, 110.0, 108.7, 57.6, 43.6, 34.3, 22.8, 22.7, 20.4. ESIMS *m/z* [M + H]⁺ 496.2; Anal. calcd. For C₂₈H₂₈F₃N₃O₂: C, 67.87; H, 5.70; N, 8.48. Found: C, 67.89; H, 5.74; N, 8.49.

5.2.6.19.

8-(1,2,3,4-Tetrahydrocyclopenta[b]indole-7-carbonyl)-2-(4-(trifluoromethyl)phenyl)-2,8-diazaspiro[4.5]decan-3-one (**6t**) White solid; yield 85%; m.p.: 196–198°C; ¹H NMR (300 MHz, DMSO-*d*₆) δ 11.03 (s, 1H), 7.87 (d, *J* = 8.5 Hz, 2H), 7.72 (d, *J* = 8.5 Hz, 2H), 7.35 (s, 1H), 7.29 (d, *J* = 8.3 Hz, 1H), 7.01 (dd, *J* = 8.2, 1.7 Hz, 1H), 3.76 (s, 2H), 3.46 (s, 4H), 2.80 (t, *J* = 6.4 Hz, 2H), 2.71 (d, *J* = 7.2 Hz, 2H), 2.57 (s, 2H), 2.49 (p, *J* = 1.9 Hz, 2H), 1.63 (s, 4H). ¹³C NMR (75 MHz, DMSO-*d*₆) δ 173.1, 170.7, 145.6, 142.8, 141.3, 126.2, 125.8, 125.7, 125.7, 123.3, 119.0, 118.8, 118.1, 117.0, 111.1, 57.6, 43.6, 34.3, 28.2, 25.2, 23.8. ESIMS *m/z* [M + H]⁺ 482.2; Anal. calcd. For C₂₇H₂₆F₃N₃O₂: C, 67.35; H, 5.44; N, 8.73. Found: C, 67.39; H, 5.47; N, 8.73.

5.2.6.20. 4-(8-(7-Methyl-1H-indazole-5-carbonyl)-3-oxo-2,8-diazaspiro[4.5]decan-2-yl)benzoic acid (**6f**)

A solution of this compound **6a** (100 mg, 0.22 mmol) in MeOH/water (1:1) (10 mL) was mixed with NaOH (2 M in water, 2 mL). The mixture was heated at 50 ° C for 1 h. The mixture was then cooled and MeOH was evaporated. The resultant was diluted with water, and acidified with 2 M aqueous HCl. The title compound was obtained by filtered as a white solid (81.4 mg, 92% yield). m.p.: 217–219°C; ¹H NMR (300 MHz, DMSO-*d*₆) δ 13.30 (s, 1H), 8.13 (s, 1H), 7.95 (d, *J* = 8.5 Hz, 2H), 7.79 (d, *J* = 8.4 Hz, 2H), 7.64 (s, 1H), 7.16 (s, 1H), 3.78 (s, 2H), 3.49 (s, 4H), 2.59 (s, 2H), 2.54 (s, 3H), 1.66 (s, 4H). ¹³C NMR (75 MHz, DMSO-*d*₆) δ 172.9, 169.6, 166.9, 143.1, 140.2, 134.4, 130.0, 128.5, 125.8, 124.7, 121.8, 120.2, 118.4, 116.9, 57.7, 43.6, 34.2, 16.7. ESIMS *m/z* [M + H]⁺ 433.1; Anal. calcd. For C₂₄H₂₄N₄O₄: C, 66.65; H, 5.59; N, 12.96. Found: C, 66.69; H, 5.64; N, 12.92.

5.3. Biological evaluation

5.3.1. In Vitro ACC1 and ACC2 Inhibition Assay.

We commissioned Pharmaron Beijing Co. Ltd., to carry out the experiments. Assay kit used is ADP-Glo™ Kinase Assay from Promega. The ADP-Glo™ Kinase Assay is a luminescent ADP detection assay to measure enzymatic activity by quantifying the amount of ADP produced during the enzymatic first half-reaction. Specifically, 4.5 μL of assay buffer containing either recombinant hACC1 (BPS Bioscience, Catalog no. 50200) or recombinant hACC2 (BPS Biosciences catalog no. 50201) were added to the wells of a 384-well Optiplat (PerkinElmer, 6007290) followed by 0.5 μL of DMSO or DMSO containing inhibitor. After 15 min incubation at room temperature, 5 μL of substrate solution was added to each well to start reaction. Final assay concentrations were 1

nM hACC1 or 0.5 nM hACC, 20 μ M ATP, 10 μ M (hACC1 assay) or 20 μ M (hACC2 assay) acetyl-CoA, 30 mM (hACC1 assay) or 12 mM (hACC2 assay) NaHCO_3 , 0.01% Brij35, 2 mM DTT, 5% DMSO, inhibitor in half-log increments between 100 μ M and 0.0017 μ M^[18]. After 60 min incubation at room temperature, 10 μ L ADP-Glo Reagent was added to terminate the reaction, and plates were incubated at room temperature for 40 min to deplete remaining ATP. Then Kinase Detection Reagent, 20 μ L, was added, and plates were incubated for 40 min at room temperature to convert ADP to ATP. ATP was measured via a luciferin/luciferase reaction using a PerkinElmer EnVision 2104 plate reader to assess luminescence.

4.2. Docking studies

For docking purposes, the crystal complex (PDB id: 4WYO) was recovered from RCSB Protein Data Bank. The docking studies were processed with the Glide docking protocol. Hydrogen atoms were added to the structure and the water was removed. Then a 60-Å box centered on the geometrical center of the ligand binding site was generated for grid calculation. All ligand molecules were drawn in ChemDraw 2014, and saved as sdf style. Then ligands were processed at a simulated pH of 7.4 ± 1.0 to generate all possible tautomers, stereoisomers, and protonation states and were finally minimized at the OPLS 2005 force field with Ligand preparation protocol of Maestro 10.2. After docking finished, only one docking conformation was saved for every compound.

4.3.2. Cell culture and proliferation inhibition assays.

The anti-proliferation activities of selected compounds were evaluated against A549, H1975, HCT116, SW620 and Caco-2 cell lines in vitro using a standard MTT assay, with **PF-1** as the positive controls. The tumor cells were seeded in 96-well plates at a concentration of 1×10^4 cells per well and cultured in RPMI 1640 medium containing 10% (v/v) fetal bovine serum, 100 U penicillin/mL and 100 mg streptomycin/mL under 5% CO_2 at 37°C for 24 h. Then 50 μ L of which containing various concentrations of compounds (triple diluted) was added and the cells were incubated for a further 48 h in FBS-free media. MTT solution was added to each well at the terminal concentration (0.5 mg/mL) followed by incubation for 4 h at 37°C. Living cells containing MTT formazan crystals were solubilized in 200 μ L DMSO. The spectrophotometric absorbance of each well was measured by a multi-detection microplate reader at a wavelength of 450 nm. The inhibition rate was calculated as $((A_{450} \text{ treated} - A_{450} \text{ blank}) / (A_{450} \text{ control} - A_{450} \text{ blank})) \times 100$. The results, expressed as IC_{50} values, was calculated by GraphPad Prism 5 statistical software.

Acknowledgements

This study was supported by the Natural Science Foundation of Jiangsu Province (No. BK20141349) and the China National Key HiTech Innovation Project for the R&D of Novel Drugs (No.2013ZX09301303-002).

References

[1] M.G. Vander Heiden, L.C. Cantley, C.B. Thompson, Understanding the Warburg effect: the

- metabolic requirements of cell proliferation, *Science*, 324 (2009) 1029-1033.
- [2] A.T. Grace Medes, Sidney Weinhouse, Metabolism of Neoplastia Tissue. IV. A Study of Lipid Synthesis in Neoplastia Tissue Slices in Vitro*, *Cancer research*, 13 (1953) 27-29.
- [3] F.V. Johannes, A. A. Elgamal, M. Eelen, I. Vercaeren, S. Joniau, H. Vanpoppel, L. Baert, K. Goddssens, W. Heyns, G. Verhoeven, Selective Activatin of The fatty acid synthesis pathway in human prostate cancer, *international journal of cancer*, 88 (2000) 176-179.
- [4] S.A. John R. Sabine, I. L Chaikoff, Control of Lipid Metabolism in Hepatomas: Insensitivity of Rate of Fatty Acid and Cholesterol Synthesis by Mouse Hepatoma BW7756 to Fasting and to Feedback Control, *Cancer research*, 27 (1967) 793-799.
- [5] R.U. Svensson, R.J. Shaw, Lipid Synthesis Is a Metabolic Liability of Non-Small Cell Lung Cancer, *Cold Spring Harbor symposia on quantitative biology*, 81 (2016) 93-103.
- [6] E. Currie, A. Schulze, R. Zechner, T.C. Walther, R.V. Farese, Jr., Cellular fatty acid metabolism and cancer, *Cell metabolism*, 18 (2013) 153-161.
- [7] J.A. Menendez, R. Lupu, Fatty acid synthase and the lipogenic phenotype in cancer pathogenesis, *Nature reviews. Cancer*, 7 (2007) 763-777.
- [8] M. Francis P. Kuhajda, Fatty-Acid Synthase and Human Cancer: New Perspectives on Its Role in Tumor Biology, *Nutrition*, 16 (2000) 202-208.
- [9] G.E. Mullen, L. Yet, Progress in the development of fatty acid synthase inhibitors as anticancer targets, *Bioorganic & medicinal chemistry letters*, 25 (2015) 4363-4369.
- [10] S. A. Comerford, Z. Huang, X. Du, Y. Wang, L. Cai, Agnes K. Witkiewicz, H. Walters, Mohammed N. Tantawy, A. Fu, H.C. Manning, Jay D. Horton, Robert E. Hammer, Steven L. McKnight, Benjamin P. Tu, Acetate Dependence of Tumors, *Cell*, 159 (2014) 1591-1602.
- [11] Z.T. Schug, B. Peck, D.T. Jones, Q. Zhang, S. Grosskurth, I.S. Alam, L.M. Goodwin, E. Smethurst, S. Mason, K. Blyth, L. McGarry, D. James, E. Shanks, G. Kalna, R.E. Saunders, M. Jiang, M. Howell, F. Lassailly, M.Z. Thin, B. Spencer-Dene, G. Stamp, N.J. van den Broek, G. Mackay, V. Bulusu, J.J. Kamphorst, S. Tardito, D. Strachan, A.L. Harris, E.O. Aboagye, S.E. Critchlow, M.J. Wakelam, A. Schulze, E. Gottlieb, Acetyl-CoA synthetase 2 promotes acetate utilization and maintains cancer cell growth under metabolic stress, *Cancer Cell*, 27 (2015) 57-71.
- [12] N. Zaidi, J.V. Swinnen, K. Smans, ATP-citrate lyase: a key player in cancer metabolism, *Cancer research*, 72 (2012) 3709-3714.
- [13] R.U. Svensson, S.J. Parker, L.J. Eichner, M.J. Kolar, M. Wallace, S.N. Brun, P.S. Lombardo, J.L. Van Nostrand, A. Hutchins, L. Vera, L. Gerken, J. Greenwood, S. Bhat, G. Harriman, W.F. Westlin, H.J. Harwood, Jr., A. Saghatelian, R. Kapeller, C.M. Metallo, R.J. Shaw, Inhibition of acetyl-CoA carboxylase suppresses fatty acid synthesis and tumor growth of non-small-cell lung cancer in preclinical models, *Nature medicine*, 22 (2016) 1108-1119.
- [14] W.P.E. Jessica E. C. Jones, Rushi Patel, Adhiraj Lanba, Nicholas B. Vera, Jeffrey A. Pfefferkorn, Cecile Vernochet*, Inhibition of Acetyl-CoA Carboxylase 1 (ACC1) and 2 (ACC2) Reduces Proliferation and De Novo Lipogenesis of EGFRvIII Human Glioblastoma Cells, *PloS one*, 12 (2017) 1-20
- [15] E. Petrova, Acetyl-CoA carboxylase inhibitors attenuate WNT and Hedgehog signaling and suppress pancreatic tumor growth, *Oncotarget*, 30 (2016) 48660-48670.
- [16] Y. Alwarawrah, P. Hughes, D. Loiselle, D.A. Carlson, D.B. Darr, J.L. Jordan, J. Xiong, L.M. Hunter, L.G. Dubois, J.W. Thompson, M.M. Kulkarni, A.N. Ratcliff, J.J. Kwiek, T.A. Haystead, Fasnall, a Selective FASN Inhibitor, Shows Potent Anti-tumor Activity in the MMTV-Neu Model of HER2(+) Breast Cancer, *Cell chemical biology*, 23 (2016) 678-688.

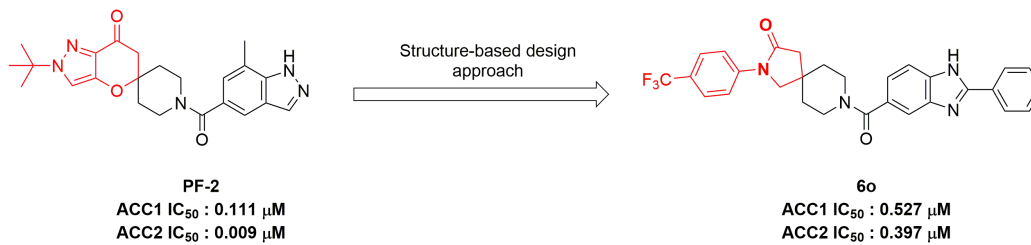
- [17] L. Tong, H.J. Harwood, Jr., Acetyl-coenzyme A carboxylases: versatile targets for drug discovery, *Journal of cellular biochemistry*, 99 (2006) 1476-1488.
- [18] G. Harriman, Acetyl-CoA carboxylase inhibition by ND-630 reduces hepatic steatosis, improves insulin sensitivity, and modulates dyslipidemia in rats, *PANS*, 113 (2016) 1796-1805
- [19] M.P. Bourbeau, A. Siegmund, J.G. Allen, H. Shu, C. Fotsch, M.D. Bartberger, K.W. Kim, R. Komorowski, M. Graham, J. Busby, M. Wang, J. Meyer, Y. Xu, K. Salyers, M. Fielden, M.M. Veniant, W. Gu, Piperazine oxadiazole inhibitors of acetyl-CoA carboxylase, *Journal of medicinal chemistry*, 56 (2013) 10132-10141.
- [20] M.P. Bourbeau, M.D. Bartberger, Recent advances in the development of acetyl-CoA carboxylase (ACC) inhibitors for the treatment of metabolic disease, *Journal of medicinal chemistry*, 58 (2015) 525-536.
- [21] T. Chonan, D. Wakasugi, D. Yamamoto, M. Yashiro, T. Oi, H. Tanaka, A. Ohoka-Sugita, F. Io, H. Koretsune, A. Hiratate, Discovery of novel (4-piperidinyl)-piperazines as potent and orally active acetyl-CoA carboxylase 1/2 non-selective inhibitors: F-Boc and triF-Boc groups are acid-stable bioisosteres for the Boc group, *Bioorganic & medicinal chemistry*, 19 (2011) 1580-1593.
- [22] C. Bengtsson, S. Blaho, D.B. Saitton, K. Brickmann, J. Broddefalk, O. Davidsson, T. Drmota, R. Folmer, K. Hallberg, S. Hallen, R. Hovland, E. Isin, P. Johannesson, B. Kull, L.O. Larsson, L. Lofgren, K.E. Nilsson, T. Noeske, N. Oakes, A.T. Plowright, V. Schnecke, P. Stahlberg, P. Sorme, H. Wan, E. Wellner, L. Oster, Design of small molecule inhibitors of acetyl-CoA carboxylase 1 and 2 showing reduction of hepatic malonyl-CoA levels in vivo in obese Zucker rats, *Bioorganic & medicinal chemistry*, 19 (2011) 3039-3053.
- [23] G.F.L. J. Denis, McGarry, D. W. Foster, Carnitine Palmitoyltransferase I The Site of Inhibition of Hepatic Fatty Acid Oxidation By Malonyl-CoA, *Journal of Biological Chemistry* 253 (1978) 4128-4136.
- [24] S. Okazaki, T. Noguchi-Yachide, T. Sakai, M. Ishikawa, M. Makishima, Y. Hashimoto, T. Yamaguchi, Discovery of N-(1-(3-(4-phenoxyphenyl)-1,2,4-oxadiazol-5-yl)ethyl)acetamides as novel acetyl-CoA carboxylase 2 (ACC2) inhibitors with peroxisome proliferator-activated receptor alpha/delta (PPARalpha/delta) dual agonistic activity, *Bioorganic & medicinal chemistry*, 24 (2016) 5258-5269.
- [25] S.W. Bagley, J.A. Southers, S. Cabral, C.R. Rose, D.J. Bernhardson, D.J. Edmonds, J. Polivkova, X. Yang, D.W. Kung, D.A. Griffith, S.J. Bader, Synthesis of 7-oxo-dihydrospiro[indazole-5,4'-piperidine] acetyl-CoA carboxylase inhibitors, *The Journal of organic chemistry*, 77 (2012) 1497-1506.
- [26] F. Zhang, G. Du, Dysregulated lipid metabolism in cancer, *World journal of biological chemistry*, 3 (2012) 167-174.
- [27] D.B. Jump, M. Torres-Gonzalez, L.K. Olson, Soraphen A, an inhibitor of acetyl CoA carboxylase activity, interferes with fatty acid elongation, *Biochemical pharmacology*, 81 (2011) 649-660.
- [28] D.A. Griffith, D.W. Kung, W.P. Esler, P.A. Amor, S.W. Bagley, C. Beysen, S. Carvajal-Gonzalez, S.D. Doran, C. Limberakis, A.M. Mathiowetz, K. McPherson, D.A. Price, E. Ravussin, G.E. Sonnenberg, J.A. Southers, L.J. Sweet, S.M. Turner, F.F. Vajdos, Decreasing the rate of metabolic ketone reduction in the discovery of a clinical acetyl-CoA carboxylase inhibitor for the treatment of diabetes, *Journal of medicinal chemistry*, 57 (2014) 10512-10526.
- [29] R. Mizojiri, M. Asano, D. Tomita, H. Banno, N. Nii, M. Sasaki, H. Sumi, Y. Satoh, Y. Yamamoto, T. Moriya, Y. Satomi, H. Maezaki, Discovery of Novel Selective Acetyl-CoA Carboxylase (ACC) 1 Inhibitors, *Journal of medicinal chemistry*, 61 (2018) 1098-1117.
- [30] D.W. Kung, D.A. Griffith, W.P. Esler, F.F. Vajdos, A.M. Mathiowetz, S.D. Doran, P.A. Amor, S.W. Bagley, T. Banks, S. Cabral, K. Ford, C.N. Garcia-Irizarry, M.S. Landis, K. Loomis, K. McPherson, M. Niosi,

K.L. Rockwell, C. Rose, A.C. Smith, J.A. Southers, S. Tapley, M. Tu, J.J. Valentine, Discovery of spirocyclic-diamine inhibitors of mammalian acetyl CoA-carboxylase, *Bioorganic & medicinal chemistry letters*, 25 (2015) 5352-5356.

[31] A.W.J.C. Paul W. Smith, R. Bell, I. J. M. Beresford, P. M. Gore, A. B. McElroy, J. M. Pritchard, V. Saez, Neil R. Taylor, R. L. G. Sheldrick, P. Ward, New spiropiperidines as potent and selective non-peptide tachykinin NK2 receptor antagonists, *Journal of medicinal chemistry*, 38 (1995) 3772-3779.

[32] P.C. Fritch, J. Krajewski, Design, syntheses, and SAR of 2,8-diazaspiro[4.5]decanones as T-type calcium channel antagonists, *Bioorganic & medicinal chemistry letters*, 20 (2010) 6375-6378.

ACCEPTED MANUSCRIPT



ACCEPTED MANUSCRIPT